

27. Gustafson, T. A., Taylor, A. & Kedes, L. *Proc. natn. Acad. Sci. U.S.A.* **86**, 2162–2166 (1989).
28. Haran, T. E., Kahn, J. D. & Crothers, D. M. *J. molec. Biol.* **244**, 135–143 (1994).
29. Pollock, R. & Treisman, R. *Genes Dev.* **5**, 2327–2341 (1991).
30. Sharrocks, A. D., Vonhesler, F. & Shaw, P. E. *Nucleic Acids Res.* **21**, 215–221 (1993).
31. Passmore, S., Maine, G. T., Elble, R., Christ, C. & Tye, B.-K. *J. molec. Biol.* **204**, 593–606 (1988).
32. Wynne, J. & Treisman, R. *Nucleic Acids Res.* **20**, 3297–3303 (1992).
33. Hagen, D. C., Bruhn, L., Westby, C. A. & Sprague, G. F. *Jr Molec. cell. Biol.* **13**, 6866–6875 (1993).
34. Sprague, G. F. *J. Adv. Genet.* **27**, 33–62 (1990).
35. Primig, M., Winkler, H. & Ammerer, G. *EMBO J.* **10**, 4209–4218 (1991).
36. Bruhn, L., Hwang Shum, J. J. & Sprague, G. F. *Jr Molec. cell. Biol.* **12**, 3563–3572 (1992).
37. Tan, S. & Richmond, T. J. *Cell* **62**, 367–377 (1990).
38. Shaw, P. E. *EMBO J.* **11**, 3011–3019 (1992).
39. Bruhn, L. & Sprague, G. F. *Jr Molec. cell. Biol.* **14**, 2534–2544 (1994).
40. Keleher, C. A., Passmore, S. & Johnson, A. D. *Molec. cell. Biol.* **9**, 5228–5230 (1989).
41. Vershon, A. K. & Johnson, A. D. *Cell* **72**, 105–112 (1993).

42. Otwinowski, Z. in *Isomorphous Replacement and Anomalous Scattering* (eds Wolf, W., Evans, P. R. & Leslie, A. G. W.) 80–86 (SERC, Daresbury, 1991).
43. Jones, T. A., Zou, J. Y., Cowan, S. W. & Kjeldgaard, M. *Acta crystallogr.* **A47**, 110–119 (1991).
44. Read, R. J. *Acta crystallogr.* **A42**, 140–149 (1986).
45. Brünger, A. *X-PLOR version 3.1 manual* (Yale Univ. Press, New Haven, CT, 1992).
46. Lavery, R. & Sklenar, H. *J. biomolec. Struct. Dyn.* **6**, 63–91 (1988).
47. Ferrin, T. E., Huang, C. C., Jarvis, L. E. & Langridge, R. *J. molec. Graph.* **6**, 13–27 (1988).
48. Liang, H. *et al. Struct. Biol.* **1**, 871–876 (1994).
49. Wolberger, C., Vershon, A. K., Liu, B., Johnson, A. D. & Pabo, C. O. *Cell* **67**, 517–528 (1991).
50. König, P. & Richmond, T. J. *J. molec. Biol.* **233**, 139–154 (1993).
51. Nurrish, S. J. & Treisman, R. *Molec. cell. Biol.* (in the press).

ACKNOWLEDGEMENTS. The plasmid containing the coding region for human SRF was provided by R. Treisman. We thank Y. Hunziker for technical assistance and D. Sargent for help with X-ray data collection. Atomic coordinates are deposited in the Brookhaven Databank.

## LETTERS TO NATURE

## Efficient photodiodes from interpenetrating polymer networks

J. J. M. Halls\*, C. A. Walsh\*, N. C. Greenham\*,  
E. A. Marseglia\*, R. H. Friend\*, S. C. Moratti†  
& A. B. Holmes†

\* Cavendish Laboratory, University of Cambridge, Madingley Road, Cambridge CB3 0HE, UK

† Melville Laboratory for Polymer Synthesis, University of Cambridge, Pembroke Street, Cambridge CB2 3RA, UK

THE photovoltaic effect involves the production of electrons and holes in a semiconductor device under illumination, and their subsequent collection at opposite electrodes. In many inorganic semiconductors, photon absorption produces free electrons and holes directly<sup>1</sup>. But in molecular semiconductors, absorption creates electron-hole pairs (excitons) which are bound at room temperature<sup>2</sup>, so that charge collection requires their dissociation. Exciton dissociation is known to be efficient at interfaces between materials with different electron affinities and ionization potentials, where the electron is accepted by the material with larger electron affinity and the hole by the material with lower ionization potential<sup>3</sup>. A two-layer diode structure can thus be used, in which excitons generated in either layer diffuse towards the interface between the layers. However, the exciton diffusion range is typically at least a factor of 10 smaller than the optical absorption depth, thus limiting the efficiency of charge collection<sup>3</sup>. Here we show that the interpenetrating network formed from a phase-segregated mixture of two semiconducting polymers provides both the spatially distributed interfaces necessary for efficient charge photogeneration, and the means for separately collecting the electrons and holes. Devices using thin films of these polymer mixtures show promise for large-area photodetectors.

Conjugated polymers have been used for thin-film semiconductor devices, including transistors<sup>4</sup> and light-emitting diodes (LEDs)<sup>5</sup>, and chemical modification of the polymer structure has allowed control of energy gap, electron affinity and ionization potential. The poly(*p*-phenylenevinylene)s, PPVs, are good hole-transporting materials and are widely used. The addition of cyano groups to a dialkoxy derivative of PPV forms the CN-PPV shown in Fig. 1, and this increases the ionization potential and electron affinity by ~0.5 eV, giving better electron injection and transport properties<sup>6</sup>. The availability of these electron- and hole-transporting polymers has allowed the fabrication of two-layer LEDs, where the electron and hole currents are controlled by the interface formed between PPV and CN-PPV<sup>7</sup>.

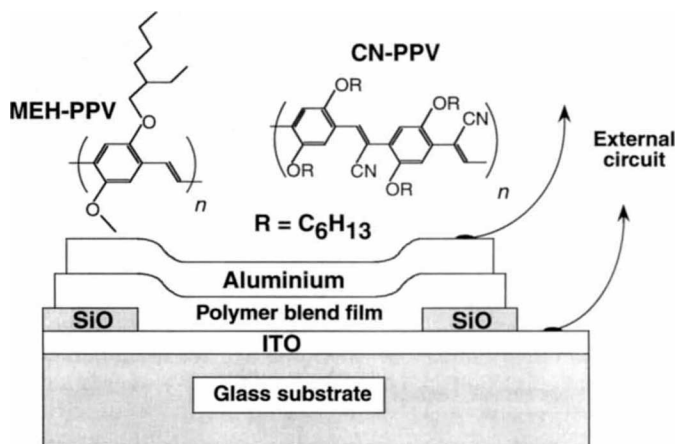
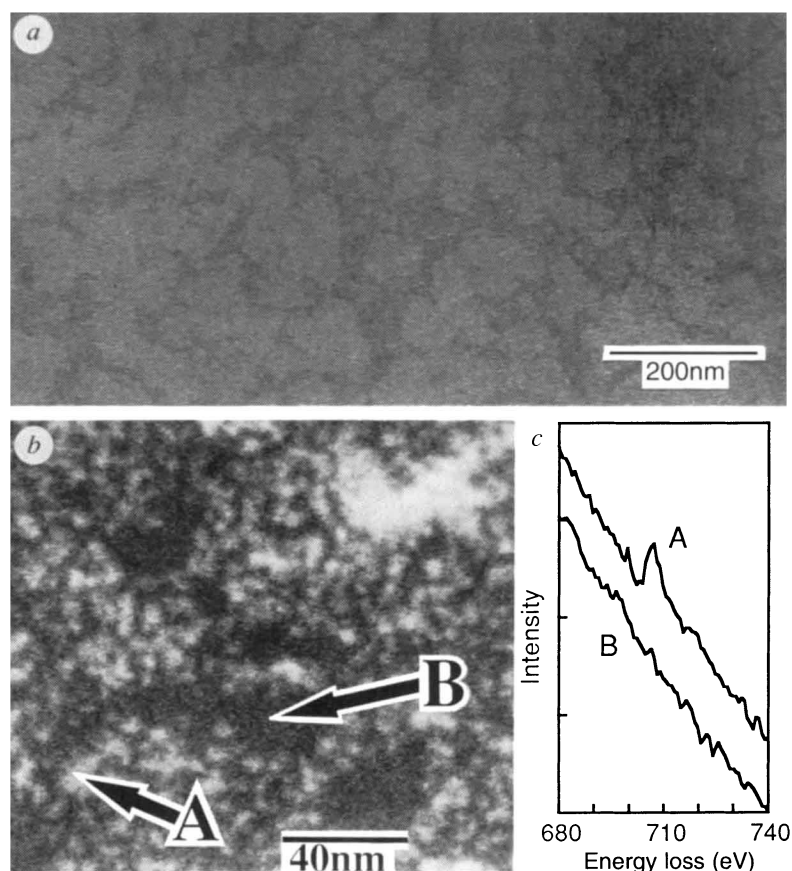


FIG. 1 Schematic diagram of the polymer photodiode, showing the two polymers used to form the interpenetrating network (ITO, indium tin oxide). The devices were fabricated by spin-coating various ratios of the polymer mixture from solution onto ITO-coated glass substrates, on which SiO insulating strips had been previously evaporated. The strips define the active area of the device and prevent short-circuits when contact is made to the electrodes. The films were annealed *in vacuo* at 100 °C for several hours to remove any residual solvent or surface contamination. Metal contacts were subsequently evaporated onto the film without breaking the vacuum.

We report here work on mixtures of a soluble PPV derivative, poly(2-methoxy-5-(2-ethylhexyloxy)-*p*-phenylenevinylene), MEH-PPV<sup>8</sup>, and CN-PPV. It is well known that mixtures of polymers tend to phase segregate on account of the low entropy of mixing<sup>9</sup>. To investigate the phase segregation of our polymer mixtures we have used a combination of transmission electron microscopy (TEM), scanning transmission electron microscopy (STEM) and parallel electron-energy-loss spectroscopy (PEELS). Thin films (~100 nm) of the mixtures were produced by spin-coating from a solution in chloroform onto a glass slide. We have used measurements of optical absorption to show that FeCl<sub>3</sub> does not dope CN-PPV but can oxidatively dope MEH-PPV throughout the thickness of these films, forming sub-gap absorption bands at 0.6 and 1.6 eV, characteristic of doped polymers of this type<sup>10</sup>. This makes it possible to stain the MEH-PPV selectively. We see clear evidence for phase separation for the whole range of compositions studied; we show here micrographs for compositions of MEH-PPV:CN-PPV of 7:1 and 1:10 (by weight) as these produce particularly clear images. The TEM bright-field image, Fig. 2a, and a STEM annular dark-field image of a mixture, Fig. 2b, clearly demonstrate that there is phase separation on the scale of 10–100 nm, as expected for films of this thickness. Performing PEELS with STEM allows

FIG. 2 *a*, Bright-field transmission electron micrograph demonstrating the presence of a phase-segregated, interpenetrating network of stained MEH-PPV (dark regions) and CN-PPV (light regions). In the annular dark-field STEM image (*b*) we associate the light regions with MEH-PPV, which is verified by the characteristic iron L-edge peak in the energy-loss spectrum (*c*) measured at position A. The dark regions do not contain iron, as shown by the spectrum from position B. Micrograph *a* was obtained from a 1:10 mixture (by weight) of MEH-PPV and CN-PPV, and micrograph *b* from a 7:1 mixture. Films were spin-coated onto glass substrates, and floated off in water onto 3-mm-diameter gold electron-microscope grids. The samples were then stained using 0.5 wt%  $\text{FeCl}_3$  solution in methanol or methanol/chloroform.



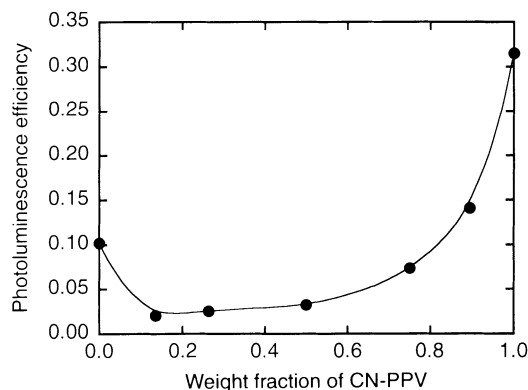
the acquisition of energy-loss spectra from areas  $\sim 1$  nm in size. From the spectra in Fig. 2c we see that iron is present only in the lighter regions of the dark-field image, showing the presence of MEH-PPV in these regions and its absence in the dark regions. The details of the microstructure are best seen in the TEM image, Fig. 2a, which shows evidence for formation of interpenetrating networks within the plane of the film.

Evidence for photoinduced charge transfer is provided by quenching of photoluminescence. Blends of MEH-PPV with the electron-acceptor fullerene,  $\text{C}_{60}$ , have been extensively investigated<sup>11,12</sup>, and show very efficient quenching (a factor of  $10^4$  for a blend of composition 1:1 by weight<sup>12</sup>), as expected for intimate mixing of donor and acceptor species. Figure 3 shows the absolute photoluminescence quantum efficiencies of a range of MEH-PPV/CN-PPV mixtures, measured using an integrating sphere<sup>13</sup>. We measured values for MEH-PPV and CN-PPV of

10% and 32% respectively, similar to values reported previously<sup>13</sup>, and found quenching to a level of around 2% to 5% for the mixtures in the composition range 1:4 to 4:1 by weight. This substantial but incomplete quenching is as expected<sup>14</sup> for an exciton diffusion range of 10 nm, given the scale of phase segregation observed in the electron micrographs shown in Fig. 2. We propose that excitons are dissociated at the dispersed interfaces by transfer of electrons to the CN-PPV and of holes to the MEH-PPV.

Photovoltaic cells were prepared with a polymer layer sandwiched between electrodes with different work functions, as used in polymer-based LEDs (Fig. 1). Figure 4a shows the current-voltage characteristics of a polymer-mixture device, both under illumination of  $0.15 \text{ mW cm}^{-2}$  at a wavelength of 550 nm, and in the dark. In the dark, the device exhibits a rectification ratio of  $10^3$  at  $\pm 3.5$  V. Under illumination, devices of this type show

FIG. 3 The absolute photoluminescence efficiency of the polymer mixture (prepared as thin (100 nm) films on quartz substrates) plotted as a function of composition. Excitation was at a wavelength of 457.9 nm. The line shown is a guide to the eye. The photoluminescence spectra of the mixtures are a combination of features due to pure MEH-PPV<sup>8</sup> and pure CN-PPV emission<sup>7</sup>.



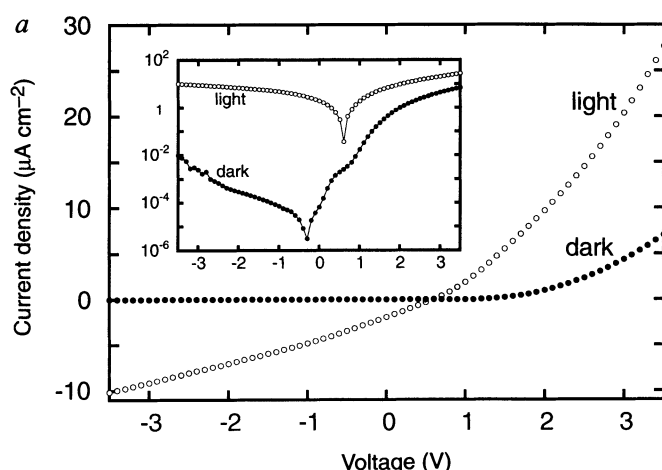
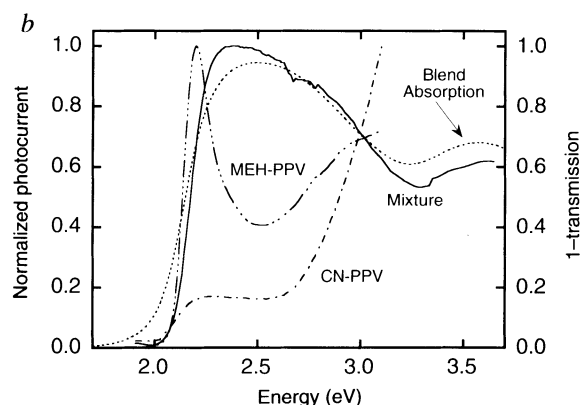


FIG. 4 a, The current-voltage characteristics of an ITO/(MEH-PPV/CN-PPV mixture)/Al device in the dark, and under illumination at a wavelength of 550 nm and intensity of  $0.15 \text{ mW cm}^{-2}$ . (Inset, the same data, with a logarithmic current axis). b, The spectral responses of the short-circuit photocurrent through an ITO/polymer/Al device. Currents have been corrected for the lamp-monochromator system response and scaled to give a peak current of unity for all devices. Intensities of



incident light were of the order of  $0.1 \text{ mW cm}^{-2}$ . The absorption spectrum of the MEH-PPV/CN-PPV film, presented as  $(1 - \text{transmission})$  for a film of the same thickness, is also shown. The polymer mixture here consisted of equal masses of the two components, but very similar results were found for mixtures of different ratios, including 7:1 and 1:10 (by weight).

a strong photoresponse, with open-circuit voltages of 0.6 V, and short-circuit currents which correspond to quantum efficiencies of up to 6%. Under forward or reverse bias, the quantum efficiencies rise rapidly, reaching 15% at a reverse bias of 3.5 V, 40% at 10 V, and considerably higher values under forward bias. These performance figures are very much better than those for similar devices made with aluminium electrodes and either MEH-PPV or CN-PPV alone. We found quantum yields of 0.04% for the short-circuit photocurrent at the peak response energy (2.2 eV) in the devices made with MEH-PPV, and of the order of  $10^{-3}\%$  for those made with CN-PPV at 2.8 eV. (Note that better efficiencies are seen for single-polymer devices if cathodes with lower work functions are employed, such as Ca and Mg<sup>15,16</sup>.)

The spectral response of photodiodes of this type provides detailed information about the device operation. Figure 4b shows the spectral dependence of the short-circuit current for devices made with the polymer mixture and with the individual polymers. We find that the spectral response of the mixture device matches the absorption (also shown in the figure) very closely, and we consider that this is excellent evidence for efficient charge generation and transport to the device electrodes. In contrast, the devices made with the individual polymers show more complicated spectral responses<sup>15,17,18</sup>. For example, the peak in response for PPV at the absorption edge is attributed to electron trapping in the photogeneration region<sup>15</sup>.

The properties of these phase-separated polymer-mixture devices are essentially different to those of devices made with polymers blended with small molecules, as exemplified by the conjugated polymer/C<sub>60</sub> blends<sup>11,12</sup>. The latter show very efficient photoinduced charge transfer, but only one of the photo-generated charges is mobile. Such blends can be used to provide unipolar transport, as exploited in some of the organic photoconductors used in xerography<sup>19</sup>. In contrast, the morphology of the phase-separated materials which we report here allows both photogenerated electrons and holes to be transported to the electrodes before recombination occurs. Collection of both carrier types is necessary for operation in a photovoltaic mode.

Polymer morphology has been used to control electronic properties in other ways. For example, Berggren *et al.*<sup>20</sup> showed that the self-organizing property of polymer mixtures can be used in polymer LEDs to obtain voltage-controlled colour sources. Also, Yang and Heeger<sup>21</sup> have used a conducting polyaniline network as a 'grid' in a polymer-based solid-state triode. An alternative approach to producing photodiodes was adopted by O'Regan *et al.*<sup>22</sup> who used sintered rutile coated with a ruthenium dye to achieve a large surface area for efficient charge dissociation. The phase-separated polymer photodiodes that we have presented here have not yet been optimized for use for solar energy conversion. However, we foresee particular interest in their use for large-area, flexible photodetectors, as required for example in medical imaging<sup>23</sup>.

*Note added in proof:* Similar measurements of photoelectric properties have recently been performed by Yu and Heeger<sup>24</sup>. □

Received 15 May; accepted 14 July 1995.

1. Bube, R. H. *Photoelectronic Properties of Semiconductors* (Cambridge Univ. Press, 1992).
2. Pope, M. & Swenberg, C. E. *Electronic Processes in Organic Crystals* (Clarendon Press, Oxford, 1982).
3. Tang, C. W. *Appl. Phys. Lett.* **48**, 183–185 (1986).
4. Burroughes, J. H., Jones, C. A. & Friend, R. H. *Nature* **335**, 137–141 (1988).
5. Burroughes, J. H. *et al.* *Nature* **347**, 539–541 (1990).
6. Moratti, S. C. *et al.* *SPIE proc. ser.* **2144**, 108–114 (1994).
7. Greenham, N. C., Moratti, S. C., Bradley, D. D. C., Friend, R. H. & Holmes, A. B. *Nature* **365**, 628–630 (1993).
8. Braun, D. & Heeger, A. J. *Appl. Phys. Lett.* **58**, 1982–1984 (1991).
9. Jones, R. A. L. *Physics World* **8**(3), 47–51 (1995).
10. Schlenoff, J. B., Obrzut, J. & Karasz, F. E. *Phys. Rev.* **B40**, 11822–11833 (1989).
11. Morita, S., Zakhidov, A. A. & Yoshino, K. *Solid St. Commun.* **82**, 249–252 (1992).
12. Sariciftci, N. S., Smilowitz, L., Heeger, A. J. & Wudl, F. *Science* **258**, 1474–1476 (1992).
13. Greenham, N. C. *et al.* *Chem. Phys. Lett.* **241**, 89–96 (1995).
14. Halls, J. J. M., Friend, R. H. & Holmes, A. B. *Synth. Metals* (in the press).

15. Marks, R. N., Halls, J. J. M., Bradley, D. D. C., Friend, R. H. & Holmes, A. B. *J. Phys. condensed Matter* **6**, 1379–1394 (1994).
16. Yu, G., Zhang, C. & Heeger, A. J. *Appl. Phys. Lett.* **64**, 1540–1542 (1994).
17. Riess, W., Karg, S., Dyakonov, V., Meier, M. & Schwoerer, M. *J. Lumin.* **60/61**, 906–911 (1994).
18. Antoniadis, H., Hsieh, B. R., Abkowitz, M. A., Jenekhe, S. A. & Stolka, M. *Synth. Metals* **62**, 265–271 (1994).
19. Borsenberger, P. M. & Weiss, D. S. *Organic Photoreceptors for Imaging Systems* (Dekker, New York, 1993).
20. Berggren, M. *et al.* *Nature* **372**, 444–446 (1994).
21. Yang, Y. & Heeger, A. J. *Nature* **372**, 344–346 (1994).
22. O'Regan, B. & Grätzel, M. *Nature* **353**, 737–740 (1991).
23. Schiebel, U. *et al.* *SPIE proc. ser.* **2163**, 129–140 (1994).
24. Yu, G. & Heeger, A. J. *J. appl. Phys.* (in the press).

ACKNOWLEDGEMENTS. We thank J. de Mello for assistance with the photoluminescence measurements, and the Polymer and Colloids group, Cavendish Laboratory, for helpful discussions. This work was supported by the UK Engineering and Physical Sciences Research Council and Philips Research, Redhill, UK.